

Article

Numerical Simulation Study on the Impact of Excavation on Existing Subway Stations Based on BIM-FEM Framework

Yi Qiu ¹, Junwei Wang ², Chao Zhang ¹, Lingxiao Hua ³ and Zhenglong Zhou ^{3,*}¹ CCCC First Highway Engineering Group Co., Ltd., Beijing 100024, China² No. 3 Engineering Co., Ltd. of CCCC First Highway Engineering Co., Ltd., Beijing 101102, China³ College of Civil Engineering, Nanjing Tech University, Nanjing 211816, China

* Correspondence: zhouzhenglong@njtech.edu.cn

Abstract: Building information modeling (BIM) and finite element method (FEM) models have a wide range of applications in underground engineering design, construction, and operation and maintenance. This study employs a BIM-FEM framework to numerically simulate the impact of excavation on existing subway stations, using the Yanjiang New City Station TOD project as a case study. This framework simplifies the smooth integration of BIM and FEM models, automating functions such as assigning material properties, conducting construction simulations, and generating high-quality meshes. Simulation results reveal significant horizontal and vertical displacements in diaphragm walls, support structures, and subway station structures, with the greatest impacts occurring closest to the excavation site. The BIM-FEM framework is validated as an effective tool for designing foundation pit support structures, enhancing numerical modeling accuracy and efficiency in underground engineering. The findings contribute to a better understanding of the dynamic interactions between excavation and underground structures, informing the development of construction strategies and protective measures to ensure structural safety.

Keywords: excavation impact; subway station structures; soil-structure interaction; structural safety; BIM-FEM



Citation: Qiu, Y.; Wang, J.; Zhang, C.; Hua, L.; Zhou, Z.. Numerical Simulation Study on the Impact of Excavation on Existing Subway Stations Based on BIM-FEM Framework. *Buildings* **2024**, *14*, 1444. <https://doi.org/10.3390/buildings14051444>

Academic Editor: Boumediene Nedjar

Received: 17 April 2024

Revised: 7 May 2024

Accepted: 10 May 2024

Published: 16 May 2024



Copyright: © 2024 by the authors. Licensee MDPI, Basel, Switzerland. This article is an open access article distributed under the terms and conditions of the Creative Commons Attribution (CC BY) license (<https://creativecommons.org/licenses/by/4.0/>).

1. Introduction

The rapid development of the economy has led to the increased importance of underground transportation systems, such as subways, in modern transportation networks. These systems effectively address the issues of traffic congestion and space limitations that arise with urban expansion. However, as urban infrastructure construction progresses, excavation projects often occur near or directly above existing underground structures [1,2]. Soil excavation can disrupt the original stress equilibrium of the site and exert complex influences on existing underground structures [3–8]. Underground structure accidents caused by external construction, such as excavation projects, are numerous [9–11], and an increasing number of researchers have recognized that the impact of excavation on existing underground structures is undeniable.

In response to this issue, numerous studies have been conducted, including site investigation [12], model testing [13], analytical approaches [14], and numerical simulation [15–18]. However, excavation projects exhibit unique characteristics and regional specificity, which affect the deformation and settlement of existing subway stations [19,20]. It is difficult to study these through traditional semi-empirical and semi-analytical methods, and the particularity of analytical methods imposes significant limitations, making it challenging to consider complex real-world conditions.

The finite element method (FEM), as a commonly used numerical simulation method, offers a more effective approach for analyzing specific engineering projects under certain conditions. This method is characterized by its ability to create detailed models based on various engineering scenarios, enabling quantitative analysis and calculation of the

interactions between underground structures and soil, as well as the actual soil conditions, while considering practical engineering circumstances. For example, Zheng et al. [21] used numerical simulation to study the influence of excavation on the settlement and deformation of existing tunnels outside the pit. Liu et al. [22] investigated the effects of the excavation process and groundwater changes on the displacement and deformation of existing tunnels using finite element numerical simulation. Wei et al. [23] combined experimental and numerical simulation methods to study the performance changes of existing tunnels under asymmetric unloading conditions in excavation projects.

However, most research has focused on the impact of excavation on existing tunnels, with relatively fewer studies conducted on the effects of excavation on the settlement and deformation of existing subway stations. Zhou et al. [11] conducted a two-dimensional simulation and analysis of the deformation characteristics and failure evolution process of a subway station under single-sided excavation based on physical model experiments and the discrete element method. However, considering the asymmetric nature of excavation and maintenance structures, two-dimensional analysis has significant limitations. Zhou et al. [24] used three-dimensional finite difference method simulations to study the effects of dewatering measures for deep excavation and subway stations on mutual settlement and deformation but did not perform refined simulations of soil parameters and maintenance structures. Li et al. [25] established a three-dimensional numerical simulation to study the effects of phased excavation of deep excavation on both sides of subway stations. Due to limitations in computational power and the complexity of modeling, most studies choose to study small two-dimensional excavations and rarely consider details of the excavation process and the arrangement of maintenance structures. However, some measures can effectively change the impact of excavation on underground structures like subway stations, and neglecting their role could significantly affect the accuracy of the final numerical computation results [26–30].

Building information modeling (BIM) originated in the construction industry; thus, existing BIM standards and applications were initially designed to meet the service conditions of the construction industry, and research in the field of excavation projects is also being conducted [31,32]. BIM has currently accelerated the digitalization process of underground space development [33,34], and numerous scholars have conducted research on interoperable methods for digital design, visualization, integration, and other characteristics using BIM [35–40]. While the aforementioned studies considered the application of BIM technology in numerical simulation and mechanical analysis of geotechnical engineering, there is limited research on excavation projects based on the BIM-FEM framework. Therefore, this paper constructs a BIM-FEM framework to numerically simulate the impact of excavation on existing subway stations, using the Yanjiang New City Station TOD project as a case study. This framework was created by Dynamo and integrated with ABAQUS, taking into account the grid requirements of geological conditions and numerical calculation analysis and simulating the entire excavation process of the foundation pit. Moreover, the numerical simulation reveals the influence of excavation on the deformation of the foundation pit support structure and subway station structure. This framework enables the transformation of data and information from the BIM model for the excavation of foundation pits to the computational model, expanding the numerical calculation functionality of foundation pit engineering BIM models.

2. Project Overview

The Yanjiang New City Station TOD project, as depicted in Figure 1, features an irregularly shaped rectangular excavation pit with depths ranging from 9.90 m to 12.917 m and a perimeter of approximately 600 m. The construction site is in close proximity to surrounding municipal roads, subway stations, high-rise buildings, and rivers, resulting in limited construction space and a complex environment. The analysis and design of the excavation and subsequent support systems are challenging because of these factors. The site's geological conditions primarily consist of silted powdered clay, silty clay, and

silty sand. Within the scope of this project's excavation, the predominant soil type is silted powdered clay, characterized by poor deformation resistance, significant creep deformation, and a marked decrease in strength after disturbance. The structural floor slab is situated in a fluid-plastic silted powdered clay layer, which poses a high risk of excavation and deformation.



Figure 1. Aerial photo of the excavation project site.

As a result, this excavation project is characterized by its large excavation depth, complex geological conditions, and complex surrounding environment. Conventional deep foundation pit support design software may not adequately assess the impact of excavation on the surrounding environment. Therefore, BIM software (Autodesk Revit2018) is utilized for fine-tuned modeling of the excavation stages and subsequent internal support systems. The professional finite element software, ABAQUS (2022), is employed to simulate the entire construction process in detail, considering the influence of complex geological conditions, foundation pit support status, and interactions between nearby existing structures on the project implementation.

3. Model Establishment

3.1. Establishment of BIM Model

Dynamo can handle a vast amount of complex geological survey data. It can generate a 3D model from the geological survey data, which can be presented in the form of a Microsoft Excel spreadsheet [41]. Furthermore, Dynamo supports secondary development using Python programming, enabling further optimization and reduction of unnecessary operations. The process of importing geological survey data into Dynamo and constructing a three-dimensional geological model involves establishing solid models of different soil layers using a layered creation approach. Specifically, this process consists of four steps, and the workflow for establishing a geological model in Dynamo is depicted in Figure 2.

Step 1: Create a node program in Dynamo that has the ability to read geotechnical report data from Excel.

Step 2: Generate an overall solid in preparation for the subsequent division (split).

Step 3: In order to obtain the contact surface between different soil layers, contour lines are generated based on the elevation data of different soil layers in Excel, e.g., Backfill, silted powdered clay, silty clay, and strongly weathered pebbly sandstone are divided into a total of four layers in the data table, and then by connecting the contour lines, a surface is

formed (surface). Starting from the top layer to the bottom layer, form a solid, and then create surfaces through each intermediate layer. Finally, perform a split to complete the solid between each pair of layers.

Step 4: Use the surfaces from Step 3 to split the solid from Step 2, generating solid models of different soil layers.

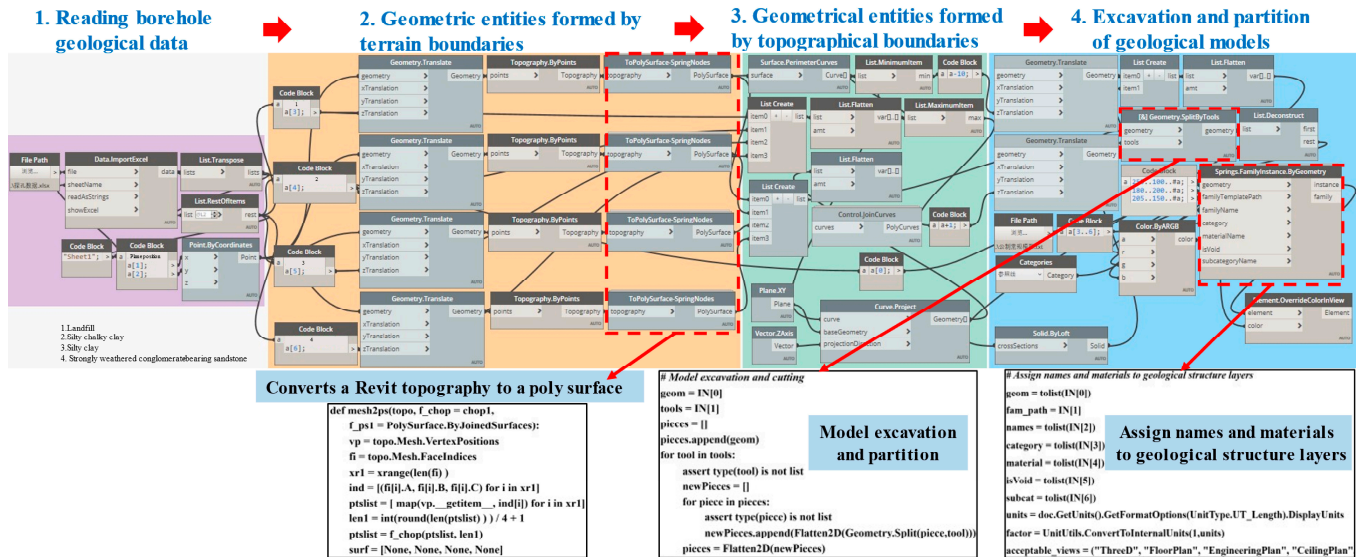


Figure 2. Workflow diagram for establishing geological models in Dynamo.

The final refined geological BIM model is presented in Figure 3. Based on the schematic diagram of the connection profile between the support structure and the existing subway support, the support structure and the existing subway support have been edited and modified. The subway station model has been constructed and integrated with the support structure and soil model. The final detailed BIM model for this project is presented in Figure 4.

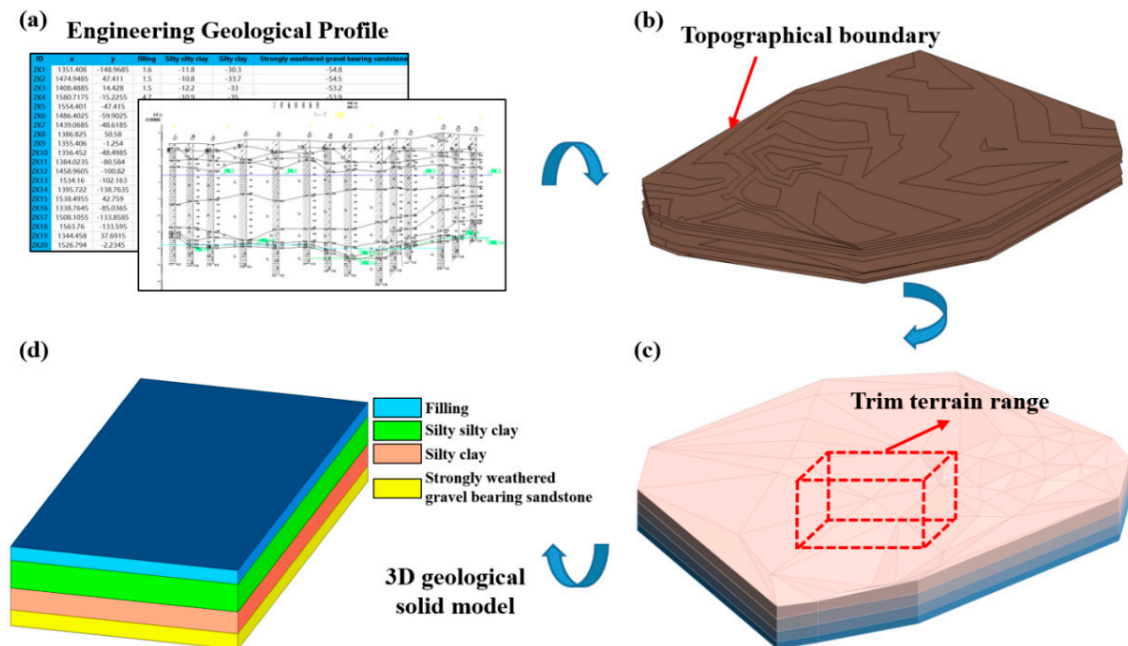


Figure 3. (a) Detailed geological information from drilling holes. (b) Generation of geological surface model. (c) Formation of geometric entities using terrain boundaries. (d) Geological model after excavation cutting.

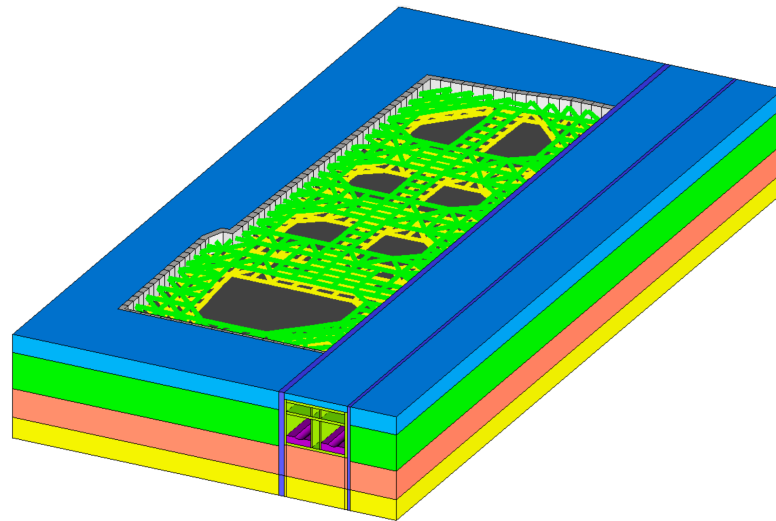


Figure 4. Detailed building information modeling (BIM) model of this project.

3.2. Establishment of ABAQUS Numerical Model

The detailed BIM model of the project is imported into ABAQUS (2022) in .stp format, enabling precise BIM-ABAQUS data interaction. This approach overcomes the shortcomings of traditional methods, such as being time-consuming and prone to errors. In case of project modifications, the model can be quickly altered and analyzed using the BIM (Autodesk Revit2018)-ABAQUS (2022) automated modeling and analysis method. The specific outcome of the BIM model imported into ABAQUS (2022) is depicted in Figure 5. Once the overall model is imported, the steel support component of the project is created using ABAQUS (2022). The layout and cross-sectional shape of the steel support are modeled based on the actual construction drawings. The steel support consists of hollow steel pipes with an outer diameter of 0.3 m, an inner diameter of 2.93 m, and a thickness of 0.07 m. The overall model, steel support, and internal structure schematic are presented in Figure 6.

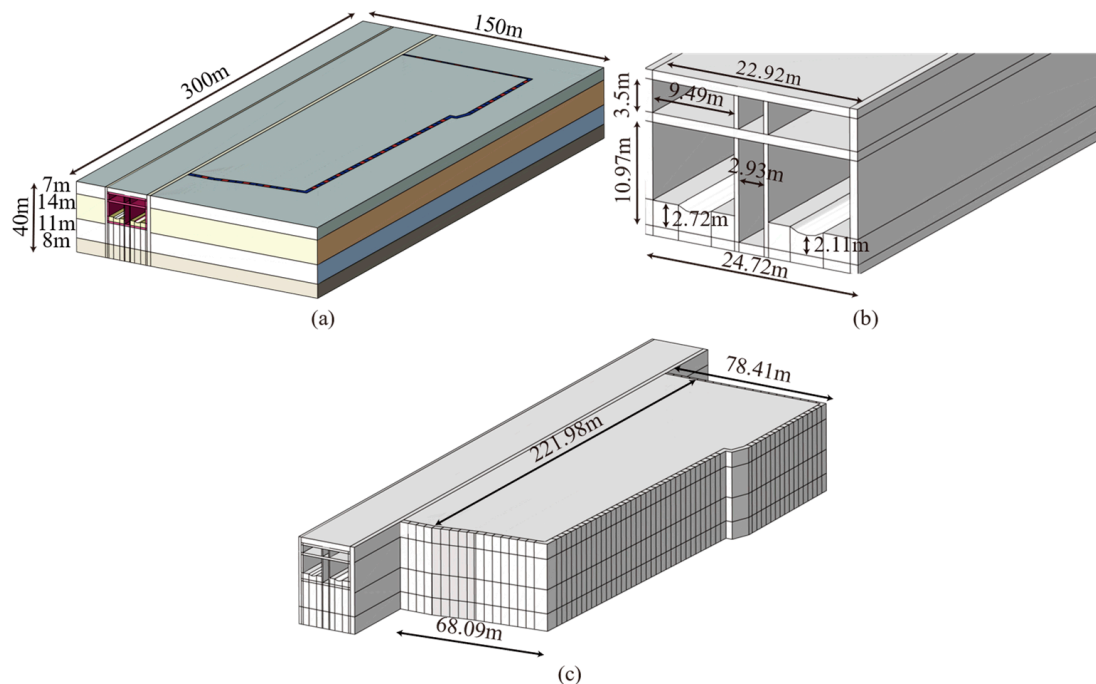


Figure 5. Schematic diagrams of the project model: (a) Overall model of the project; (b) Subway station structures; (c) Retaining structures.

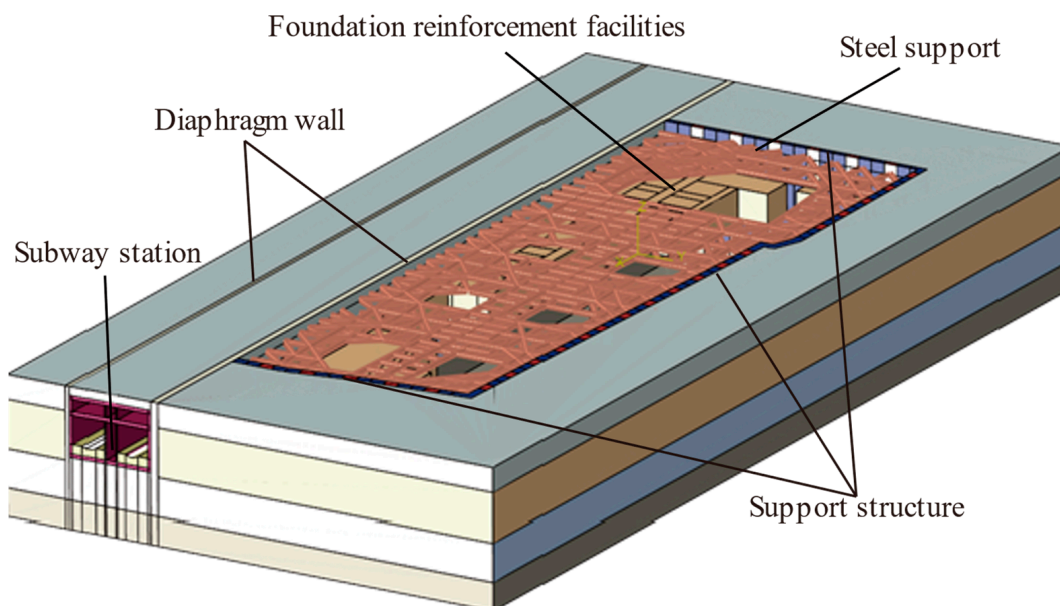


Figure 6. Artistic representation of steel supports and internal structures.

3.2.1. Subsection

The geologic model consists of four soil layers, and parameters for each layer can be obtained from field geologic surveys and summarized in an engineering geology report for modeling options. Soil is characterized using the Mohr–Coulomb constitutive model; soil layer parameters include: layer thickness, elastic modulus, Poisson’s ratio, density, cohesion, internal friction angle, dilatancy angle. The foundation pit excavation process involves numerous complex soil–structure interactions, thus requiring careful consideration in establishing the soil constitutive model and parameters. When the deformation resulting from foundation pit excavation is relatively minor, and the stress level is low, the soil’s nonlinear behavior may not be significant. Taking into account the model’s overall size and the complexity of the structural details while ensuring a certain level of calculation accuracy and efficiency, the elastic–plastic model for soil simulation can more effectively capture soil nonlinear behavior, as well as the variation trends and extreme values of the structure, soil forces, and deformation. Consequently, soil, foundation pit support, steel supports, ground consolidation, and Subway station structures are characterized using a linear elasticity constitutive model. The material parameters used in the model are provided in Table 1.

Table 1. Basic physical and mechanical parameters of surrounding rock and structural materials.

Name	Layer Thickness D (m)	Elastic Modulus E (MPa)	Poisson’s Ratio	Density (kg/m ³)	Cohesion c (kPa)	Internal Friction Angle φ' (°)	Dilatancy Angle ψ (°)
Backfill	7	5	0.3	1900	20	10	0
Silted powdered clay	14	3	0.32	1830	50	15	0
Silty clay	11	4.6	0.28	1900	60	25	0
Strongly weathered pebbly sandstone	8	43	0.24	2200	1000	30	5
Subway station structures	-	3.15×10^4	0.2	2500	-	-	-
Steel supports	-	2×10^5	0.3	7850	-	-	-
Underground continuous wall	-	3.15×10^4	0.2	2500	-	-	-
Row of piles	-	3.15×10^4	0.2	2500	-	-	-
Strengthening piles	-	3.45×10^4	0.2	2500	-	-	-
Ground consolidation	-	3.15×10^4	0.2	2500	-	-	-

3.2.2. Simulation of Actual Excavation Process

In the foundation pit excavation process, geostatic stress equilibrium is first conducted to eliminate the pressures and settlement deformation generated in the soil due to its own

gravity and other additional pressures after long-term deposition. The process for geostatic stress equilibrium is as follows.

(1) Static calculation: Establish the necessary model components and assign the corresponding material properties, contact relationships, earth pressure, and gravitational forces. Restrict the horizontal displacement on both the left and right sides, apply fixed constraints for both horizontal and vertical directions at the base rock surface, and apply vertical gravitational forces. Perform the calculation using the Static, General step to obtain the Open Document Database (ODB) file containing the results.

(2) Repeat the geostatic stress equilibrium by importing the ODB file, select the Stress type in the Predefined Field, and choose the soil portion for the calculation. Input the appropriate Step and increment numbers from the calculation ODB file and perform the static calculation again. After four iterations, if the vertical displacement of the soil and underground structures in the calculation results approaches 10^{-4} , it is considered that the geostatic stress equilibrium has been achieved. The flowchart illustrating the calculation process is presented in Figure 7.

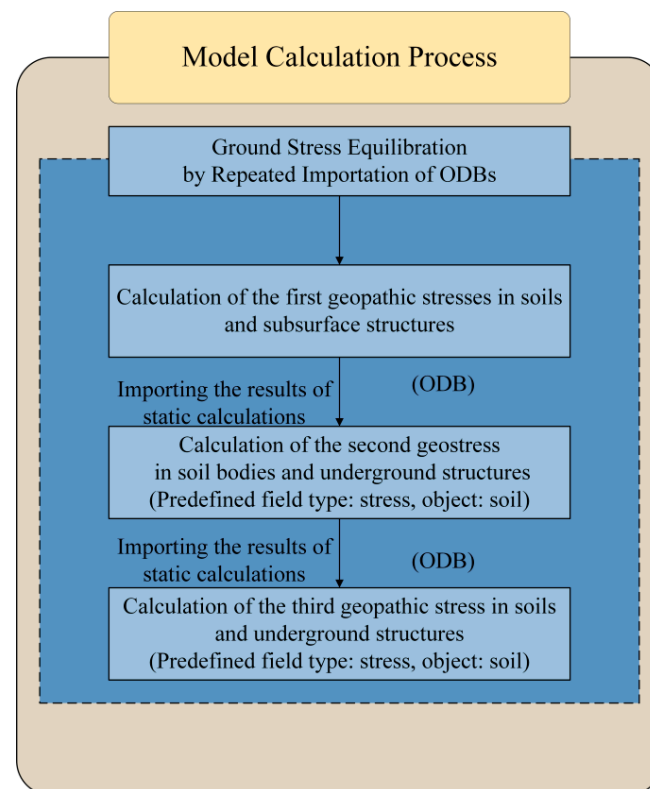


Figure 7. Schematic flowchart for geostatic stress equilibrium calculation.

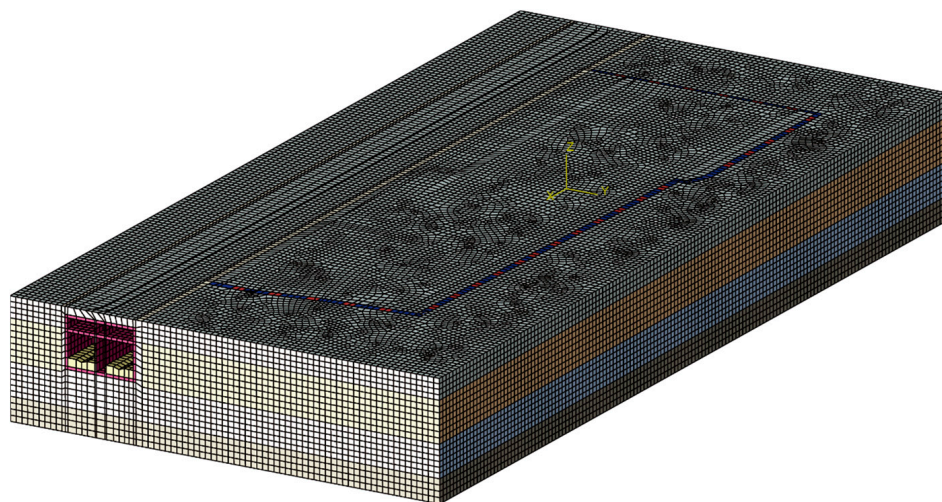
In the foundation pit excavation simulation, the stratified excavation process is refined. The entire excavation process is divided into three stages, with excavation depths of 3 m, 3 m, and 4 m for each layer, respectively, to more accurately simulate the actual construction excavation and gain a more comprehensive understanding of the impact of foundation pit excavation on the surrounding environment. Furthermore, the birth–death element concept in ABAQUS (2022) is utilized to simulate the entire process of staged excavation and steel support installation. During the simulation of the dynamic foundation pit excavation process, the response of the foundation pit and surrounding structures at various excavation stages can also be analyzed. Existing Subway station structures, underground continuous walls, pile foundations, and other nearby structures are modeled, taking into account the mutual influence between the construction process and these structures during the excavation. The specific simulation process is provided in Table 2.

Table 2. Simulation process of the entire foundation pit excavation.

Step	Simulation Content
Step 1	Repeat the import of ODB to achieve geostatic stress equilibrium
Step 2	Arrange two layers of steel supports at the corresponding locations, but do not activate them temporarily
Step 3	Excavate the first layer of soil with a depth of 3 m
Step 4	Activate the first layer of steel supports
Step 5	Excavate the second layer of soil with a depth of 3 m
Step 6	Activate the second layer of steel supports
Step 7	Excavate the third layer of soil with a depth of 4 m and perform ground consolidation

3.2.3. Contact Setup and Meshing

Contacts include the nodes in contact between the steel supports and the cover slabs, the contact between the retaining structure and the cover slabs, and the inner side of the retaining structure. Both interfaces are set with Tie constraints, with the primary interface being the contact between the steel supports and the retaining structures, and the secondary interfaces being the cover slabs and the inner sides of the retaining structures. Due to the irregular rectangular foundation pit and the irregular shape of the existing tunnels, the difficulty of meshing is relatively high. Therefore, priority is given to cutting the subway station structures and those close to the foundation pit. The schematic diagram of mesh division after cutting is shown in Figure 8. The model dimensions are 300 m × 150 m × 40 m. The grid types for soil, foundation pit support, ground reinforcement, and subway station structures are hexahedral meshes, with element types C3D8R, totaling 260,106 elements. The steel supports are simulated with Beam elements, using 502 three-dimensional two-node beam elements (B31) and 280 nodes.

**Figure 8.** Mesh division effect picture.

4. Finite Element Analysis Based on the Entire Process of Foundation Pit Excavation

In general, foundation pit excavation is divided into multiple excavation steps, each of which has a significant impact on surrounding buildings and underground structures. By using ABAQUS (2022) software and employing different analysis steps and birth–death elements to simulate the entire construction process of the foundation pit excavation, the horizontal displacement (U2) contour map, vertical displacement (U3) contour map, and Mises stress contour map of the overall model after the third layer of excavation are shown in Figure 9. The horizontal movement of the foundation pit is mainly the lateral shift away from the subway station side of the pit, which is concentrated in the central position of each diaphragm wall and decreases parabolically towards both sides. The vertical displacement

of the foundation pit is primarily due to soil settlement at the base. The Mises stress distribution of the support structure is relatively uniform and mainly concentrated in the areas where the foundation pit and the retaining structure come into contact. Based on the model calculation results, this paper extracts the displacement and stress structure of each part of the model and analyzes the deformation of the foundation pit, support structure, and auxiliary structure of the subway station during the entire excavation process.

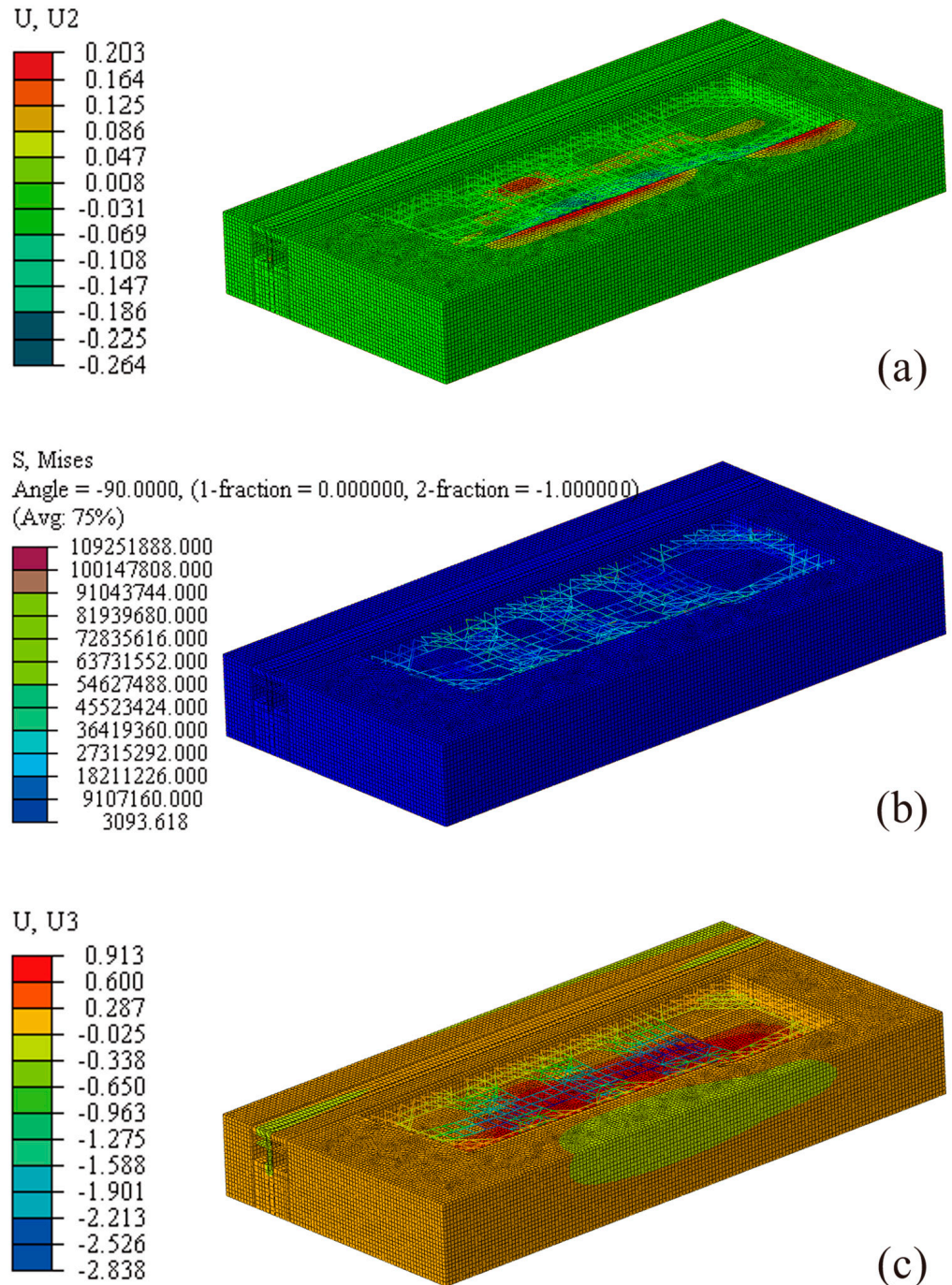


Figure 9. Post-excavation model data diagrams. (a) Horizontal displacement (unit: m). (b) Vertical displacement (unit: m). (c) Mises stress (unit: Pa).

4.1. Deformation Analysis of the Foundation Pit and Support Structure

To monitor the settlement deformation of the soil above the subway station and analyze the deformation values at different distances from the top soil to the diaphragm wall, the orientation of the foundation pit monitoring points is shown in Figure 10. The vertical displacement results of the top soil at the top of the diaphragm wall with the excavation progress are shown in Figure 11. The horizontal coordinate represents the excavation analysis step, and the vertical coordinate represents the displacement value of the top soil. The colored broken lines represent the distance of the top soil from the side close to the foundation pit. It can be observed that as the excavation progresses, the soil around the foundation pit gradually bulges upward, and the closer to the side of the foundation pit, the larger the displacement value, reaching 81.5 mm. This is because as the foundation pit is excavated, the horizontal confinement around the soil gradually decreases, allowing the pore water pressure in the soil to be released, causing the soil to expand upward.

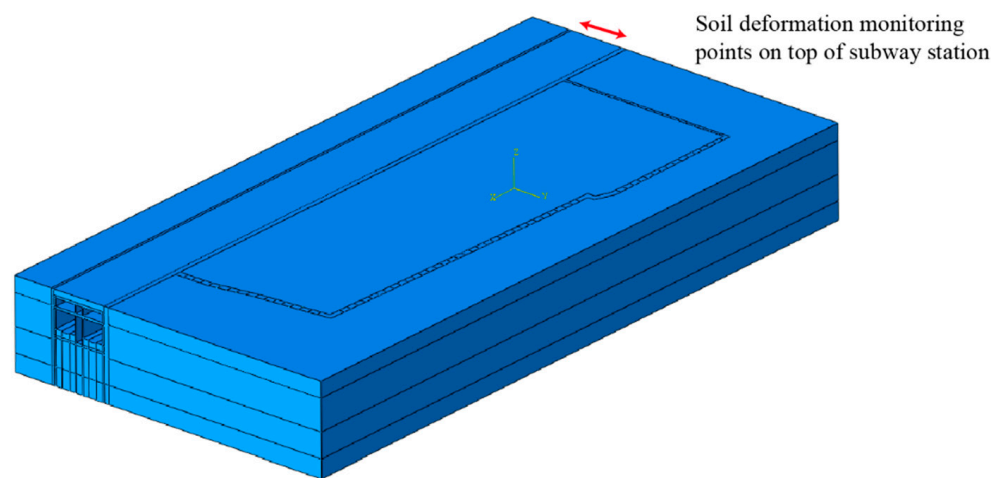


Figure 10. Orientation of the monitoring points at the subway station.

To monitor the deformation of diaphragm walls and foundation pit support, the horizontal displacement of the diaphragm walls and the support structure near Yan Ya Yuan 24F was analyzed. The deformation cloud diagram and monitoring points of the diaphragm walls and pit support at -10 m excavation depth are shown in Figure 12. The simulated horizontal displacement results for the diaphragm walls and the support structure near Yan Ya Yuan 24F are shown in Figure 13. In these figures, the horizontal axis represents the horizontal displacement, and the vertical axis represents the burial depth (the vertical distance of the monitoring points from the ground surface). It can be observed that as the burial depth increases, the horizontal displacement of the diaphragm walls and support structures first increases and then decreases. The maximum horizontal displacement of the diaphragm walls on both sides occurs at a burial depth of 22 m, with the maximum values for the diaphragm walls close to and away from the foundation pit being 64.9 mm and 59.6 mm, respectively. The larger maximum horizontal displacement of the diaphragm walls near the foundation pit indicates a greater impact from the excavation on structures closer to the pit. The maximum horizontal displacement of the support structure near Yan Ya Yuan 24F occurs at a burial depth of 27 m, with a value of 106.5 mm.

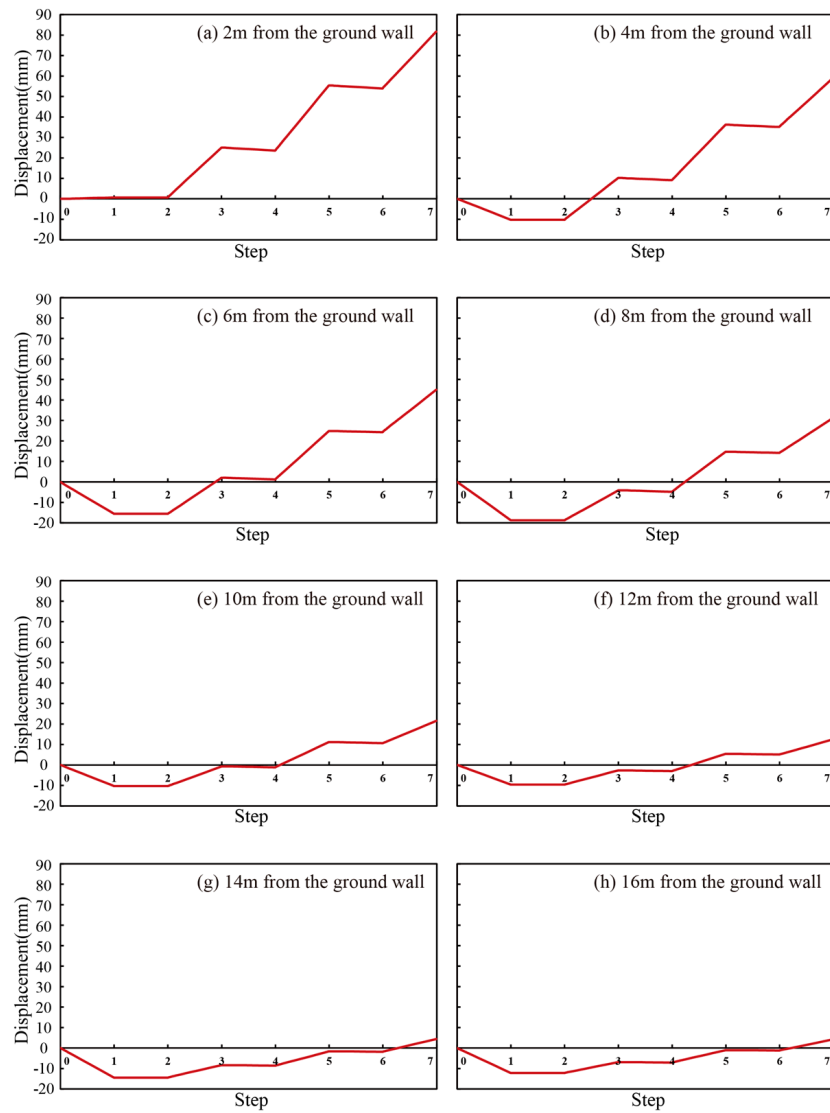


Figure 11. Vertical displacement diagram of the top soil of the diaphragm wall with the foundation pit excavation progress.

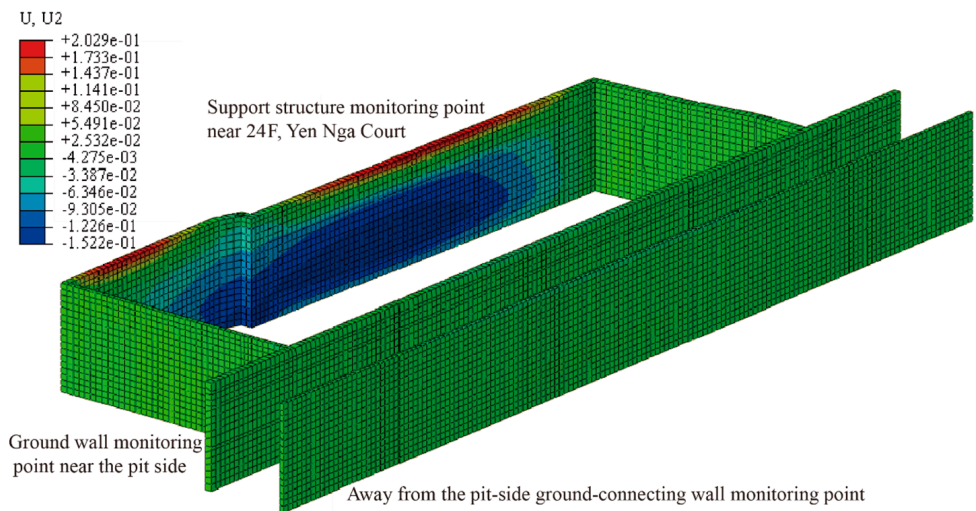


Figure 12. Contour plot of horizontal displacement (U2) of diaphragm walls and foundation pit support (unit: m).

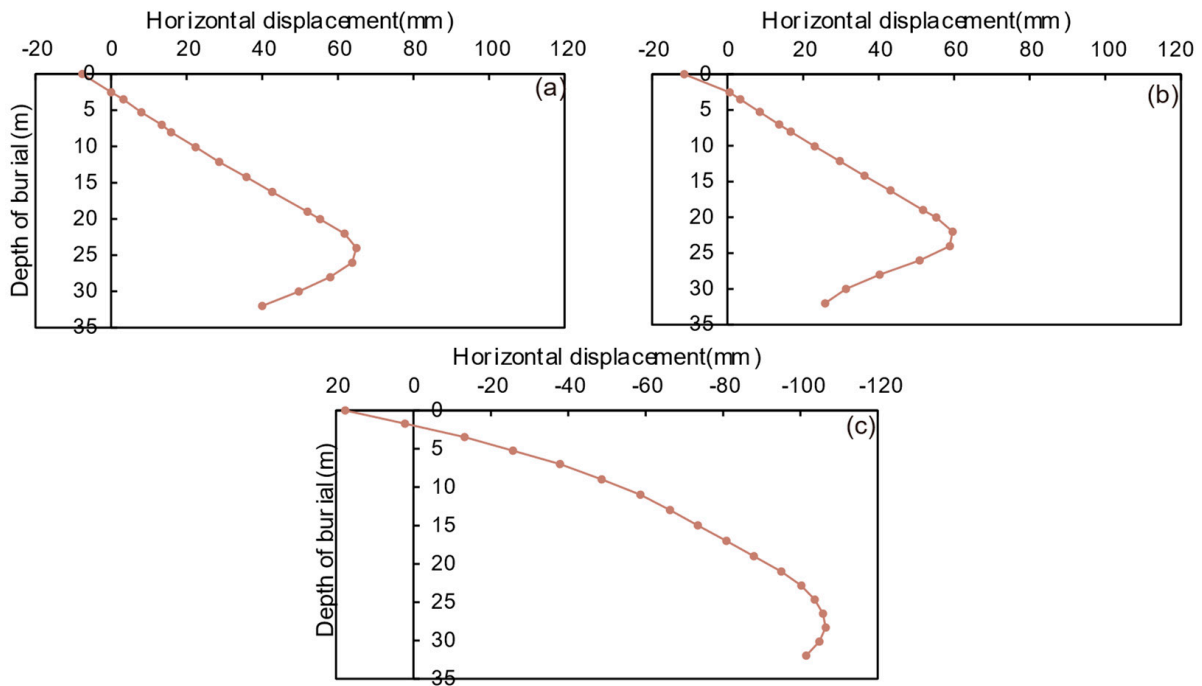


Figure 13. Structural horizontal displacement diagrams. (a) Diaphragm wall on the side near the foundation pit. (b) Diaphragm wall on the side away from the foundation pit. (c) Support structure near Yan Ya Yuan 24F.

4.2. Deformation Analysis of Subway Station Structures

To analyze the impact of foundation pit excavation on subway station structures, the displacement at multiple locations of the subway station structures was analyzed. The horizontal displacement contour diagrams of the subway station structures after the foundation pit excavation and the layout diagram of the monitoring points for the subway station structures are shown in Figure 14, and the arrangement of the monitoring points for the subway station structures is shown in Figure 15.

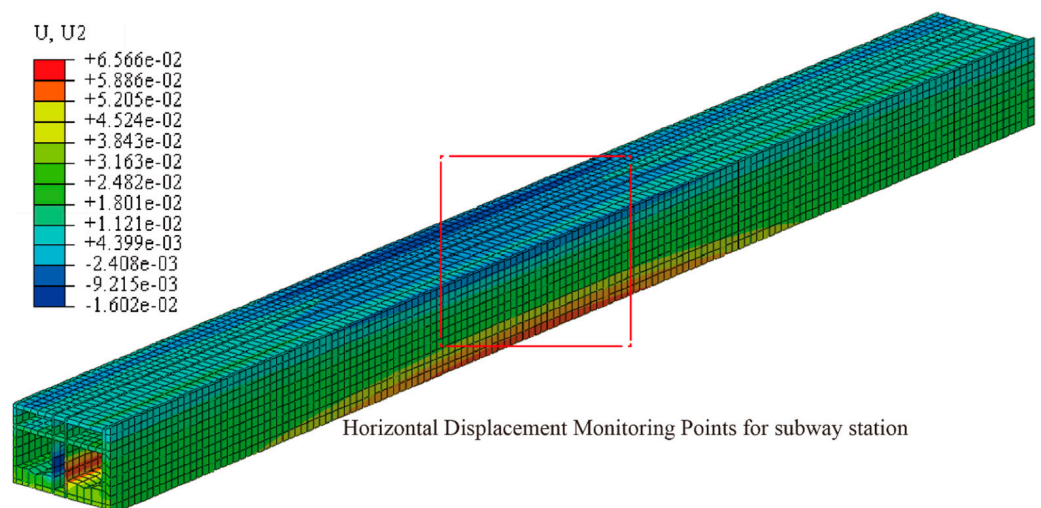


Figure 14. Horizontal displacement (U2) contour diagram of the subway station structures after foundation pit excavation (unit: m).

The horizontal displacement results of the subway structure during pit excavation are shown in Figures 16 and 17. The horizontal coordinates indicate the excavation analysis step, and the vertical coordinates indicate the deformation value of the subway structure. It can be seen that as the excavation proceeds, the subway structures are all shifted toward the pit side. The maximum horizontal displacement of the subway structure close to the pit side occurs at C7, which is 55.3 mm, and the maximum horizontal displacement of the subway ancillary structure away from the pit side occurs at D7, which is 54.5 mm.

The results of vertical displacement of subway station structures during foundation pit excavation are displayed in Figures 18 and 19. The horizontal axis indicates the excavation analysis step, while the vertical axis shows the deformation value of the subway station structures. It can be seen that as the excavation proceeds, subway station structures on the side near the foundation pit exhibit varying degrees of upward displacement. The maximum vertical displacement of the tunnel near the pit occurs at C5, amounting to 78.5 mm. The subway station structures D1 and D4 on the near side of the pit exhibit different degrees of downward displacement, which are -1.2 mm and -5.4 mm, respectively. The maximum upward vertical displacement of the subway station structures on the far side of the pit occurs at D6, reaching 13.44 mm. The vertical displacement of subway station structures near the foundation pit is much larger than that of the tunnel on the far side, indicating that the structures closer to the pit are more significantly affected by the pit construction.

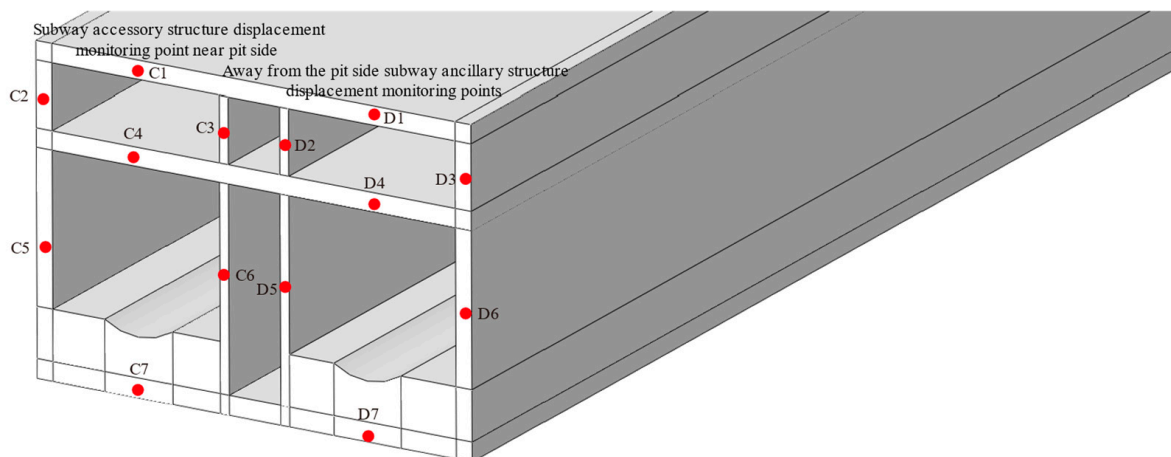


Figure 15. Layout diagram of monitoring points for subway station structures.

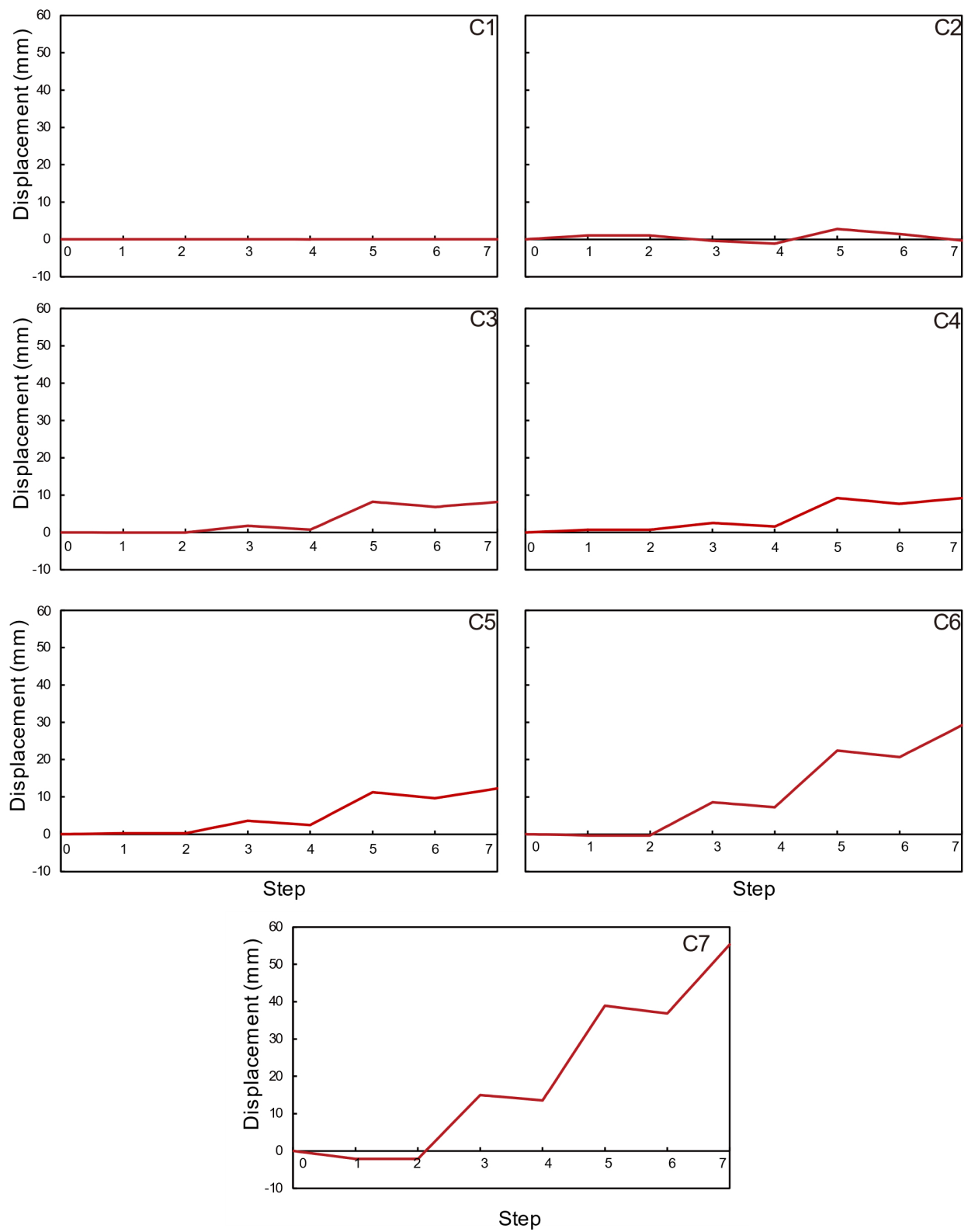


Figure 16. Horizontal displacement of subway station structures on the side close to the foundation pit.

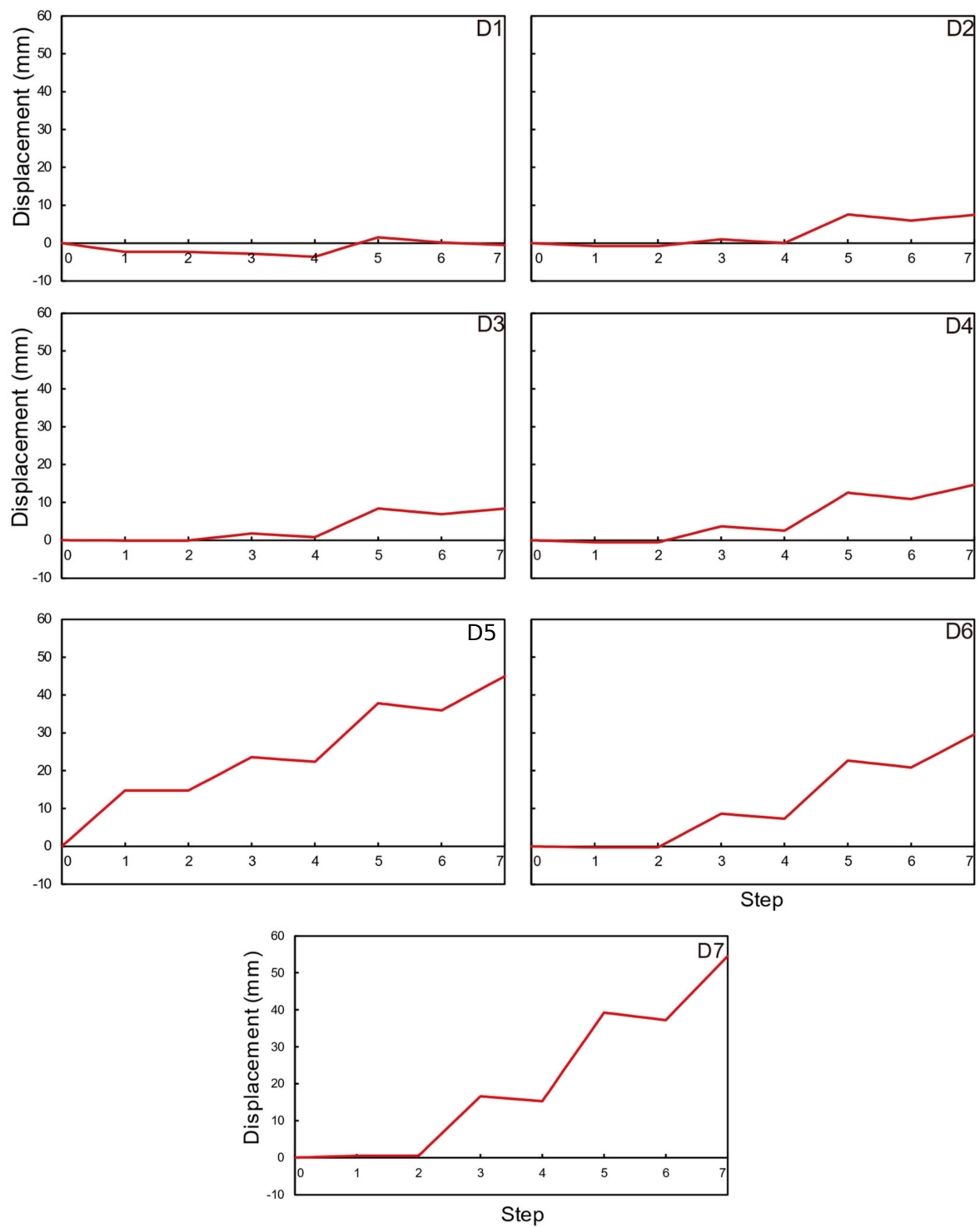


Figure 17. Horizontal displacement of subway station structures on the side away from the foundation pit.

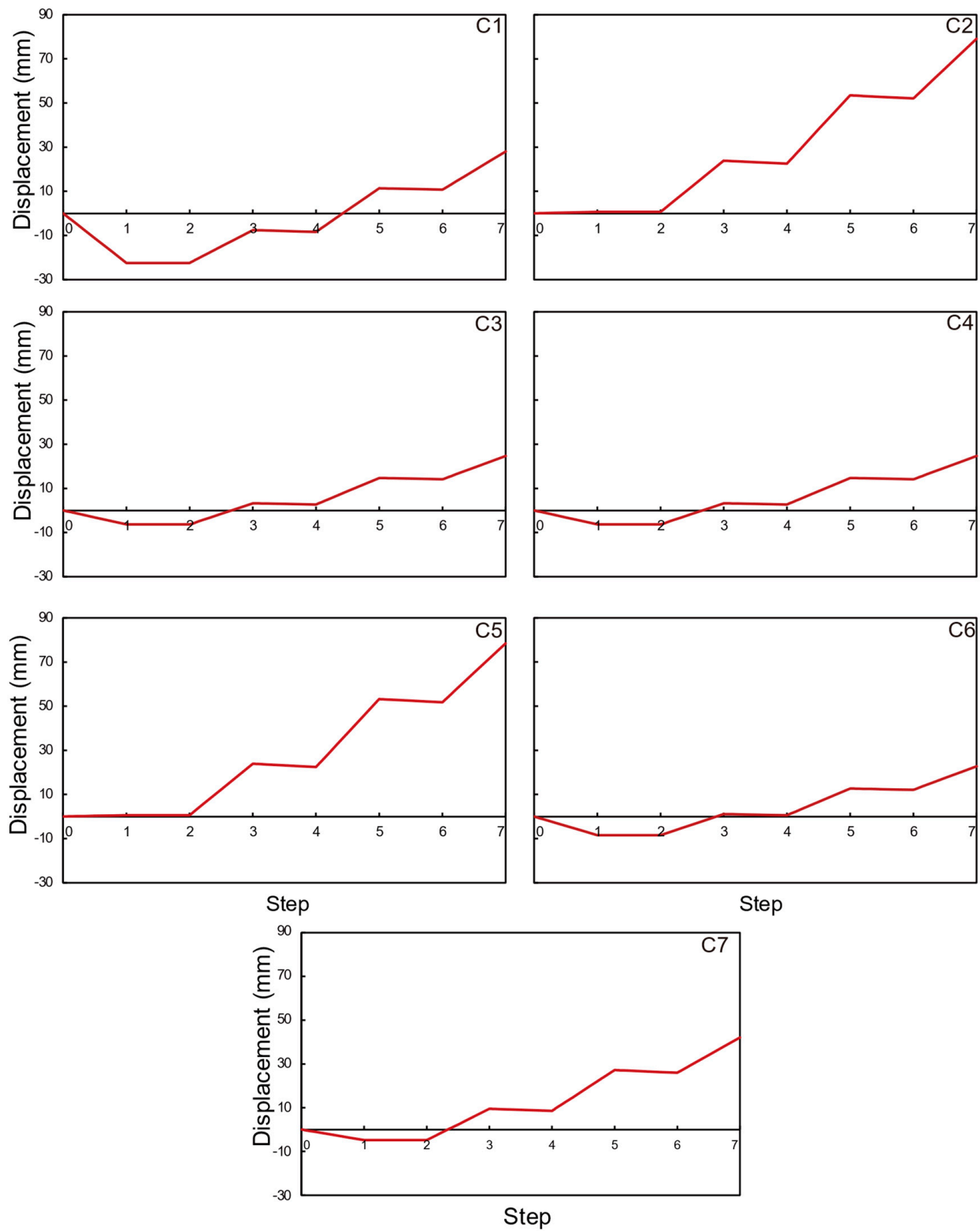


Figure 18. Vertical displacement of subway station structures on the side close to the foundation pit.

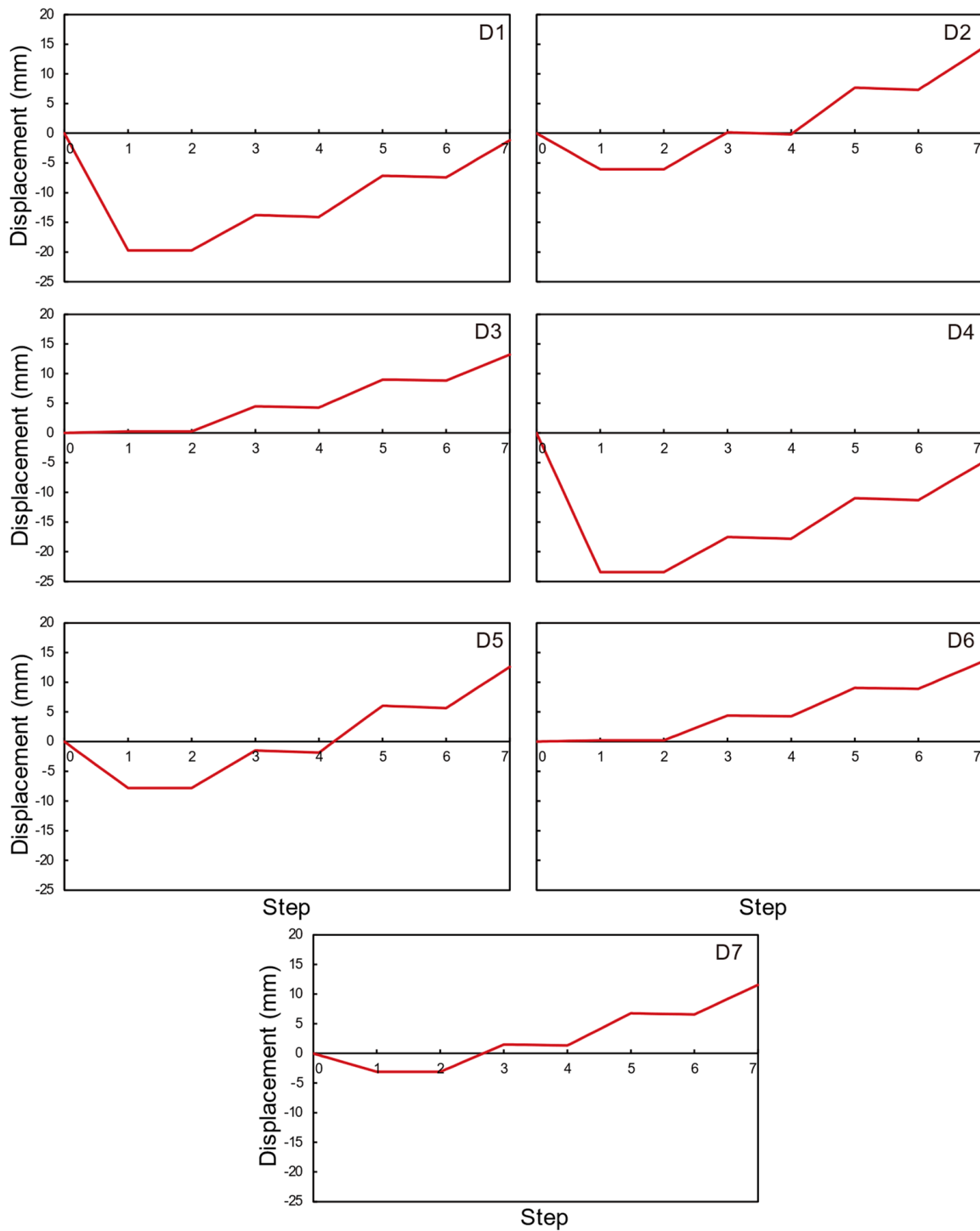


Figure 19. Vertical displacement of subway station structures on the side away from the foundation pit.

5. Conclusions

At present, there is no complete data interface between BIM software and geotechnical engineering calculation software. Non standardized geometric BIM models such as geotechnical and underground structures, are often converted into finite element models, which cannot meet the requirements of refined safety analysis of underground structures. This paper presents the establishment of a three-dimensional finite element model for the Yanjiang New City TOD project above the subway station through the BIM-FEM integration.

While ensuring the accuracy of the model, fine mesh division is carried out to simulate the deformation of adjacent subway stations during the entire excavation process of the foundation pit. The specific research conclusions are as follows.

(1) Through the Autodesk Revit software platform and based on Dynamo visualization programming technology, a series of node package programs are developed to import drilling data into Dynamo, set appropriate modeling data ranges, efficiently create geological BIM models, and combine them with the BIM models of subway stations to efficiently create three-dimensional models of geology and subway stations.

(2) Intelligent analysis of excavation of adjacent subway station structural foundation pits is achieved through numerical simulation based on the BIM-FEM framework. While ensuring calculation accuracy, this method can analyze multiple construction process scenarios, obtain more comprehensive underground structure analysis data, and observe more local structural details.

(3) Case analysis shows that as the foundation pit is gradually excavated, the horizontal confining pressure on the surrounding soil gradually decreases, and the soil around the foundation pit gradually rises upwards. The displacement value on the side closer to the foundation pit is greater. As the burial depth increases, the horizontal displacement of the diaphragm wall and support structure first increases and then decreases. The subway structure experiences displacement in both horizontal and vertical directions, and the displacement generated by the subway structure on the side closer to the foundation pit is greater.

This work demonstrates the feasibility and effectiveness of simulating deep excavation of adjacent subway pits based on the BIM-FEM framework. However, due to the lack of on-site monitoring data for comparative analysis, in the future, a large amount of system monitoring data can be combined to promote model calibration of adjacent subway deep foundation pit excavation and improve the robustness and universality of the workflow.

Author Contributions: Conceptualization, J.W.; methodology, J.W. and L.H.; validation, Z.Z.; investigation, J.W.; data curation, Y.Q.; writing—original draft preparation, Y.Q.; writing—review and editing, L.H. and Z.Z.; visualization, Y.Q.; supervision, J.W., C.Z. and Z.Z.; project administration, C.Z. All authors have read and agreed to the published version of the manuscript.

Funding: This research received no external funding.

Data Availability Statement: The original contributions presented in the study are included in the article, further inquiries can be directed to the corresponding author.

Conflicts of Interest: Authors Yi Qiu and Chao Zhang were employed by the company CCCC First Highway Engineering Group Co., Ltd. Author Junwei Wang was employed by the company No. 3 Engineering Co., Ltd. of CCCC First Highway Engineering Co., Ltd. The remaining authors declare that the research was conducted in the absence of any commercial or financial relationships that could be construed as a potential conflict of interest.

References

1. Meng, F.Y.; Chen, R.P.; Xu, Y.; Wu, K.; Wu, H.N.; Liu, Y. Contributions to responses of existing tunnel subjected to nearby excavation: A review. *Tunn. Undergr. Space Technol.* **2022**, *119*, 104195. [[CrossRef](#)]
2. Vinoth, M.; MS, A. Behaviour of existing tunnel due to adjacent deep excavation—A review. *Int. J. Geotech. Eng.* **2022**, *16*, 1132–1151. [[CrossRef](#)]
3. Liyanapathirana, D.S.; Nishanthan, R. Influence of deep excavation induced ground movements on adjacent piles. *Tunn. Undergr. Space Technol.* **2016**, *52*, 168–181. [[CrossRef](#)]
4. Luo, Z.; Das, B.M. System probabilistic serviceability assessment of braced excavations in clays. *Int. J. Geotech. Eng.* **2016**, *10*, 135–144. [[CrossRef](#)]
5. Huang, F.; Zhang, M.; Wang, F.; Ling, T.; Yang, X. The failure mechanism of surrounding rock around an existing shield tunnel induced by an adjacent excavation. *Comput. Geotech.* **2020**, *117*, 103236. [[CrossRef](#)]
6. Meng, F.Y.; Chen, R.P.; Xie, S.W.; Wu, H.N.; Liu, Y.; Lin, X.T. Excavation-induced arching effect below base level and responses of long-collinear underlying existing tunnel. *Tunn. Undergr. Space Technol.* **2022**, *123*, 104417. [[CrossRef](#)]
7. Soomro, M.A.; Mangnejo, D.A.; Saand, A.; Mangi, N.; Auchar Zardari, M. Influence of stress relief due to deep excavation on a brick masonry wall: 3D numerical predictions. *Eur. J. Environ. Civ. Eng.* **2022**, *26*, 7621–7644. [[CrossRef](#)]

8. Zhao, Y.; Chen, X.; Hu, B.; Huang, L.; Lu, G.; Yao, H. Automatic monitoring and control of excavation disturbance of an ultra-deep foundation pit extremely adjacent to metro tunnels. *Tunn. Undergr. Space Technol.* **2023**, *142*, 105445. [[CrossRef](#)]
9. Chen, R.; Meng, F.; Li, Z.; Ye, Y.; Ye, J. Investigation of response of metro tunnels due to adjacent large excavation and protective measures in soft soils. *Tunn. Undergr. Space Technol.* **2016**, *58*, 224–235. [[CrossRef](#)]
10. Li, T.X.; Xi, W.Y. Cause analysis on damage of adjacent metro shield tunnel due to deep pit excavation with pile-anchor retaining. *J. Railw. Eng. Soc.* **2016**, *33*, 109–115.
11. Zhou, F.; Zhou, P.; Li, J.; Lin, J.; Ge, T.; Deng, S.; Ren, R.; Wang, Z. Deformation characteristics and failure evolution process of the existing metro station under unilateral deep excavation. *Eng. Fail. Anal.* **2022**, *131*, 105870. [[CrossRef](#)]
12. Meng, F.Y.; Chen, R.P.; Wu, H.N.; Xie, S.W.; Liu, Y. Observed behaviors of a long and deep excavation and collinear underlying tunnels in Shenzhen granite residual soil. *Tunn. Undergr. Space Technol.* **2020**, *103*, 103504. [[CrossRef](#)]
13. Cheng, X.; Hong, T.; Lu, Z.; Cheng, X. Characterization of underlying twin shield tunnels due to foundation-excavation unloading in soft soils: An experimental and numerical study. *Appl. Sci.* **2021**, *11*, 10938. [[CrossRef](#)]
14. Huang, M.; Li, H.; Yu, J.; Zhang, C.; Ni, Y. On the simplified method for evaluating tunnel response due to overlying foundation pit excavation. *Transp. Geotech.* **2023**, *42*, 101048. [[CrossRef](#)]
15. Li, M.G.; Chen, J.J.; Wang, J.H.; Zhu, Y.F. Comparative study of construction methods for deep excavations above shield tunnels. *Tunn. Undergr. Space Technol.* **2018**, *71*, 329–339. [[CrossRef](#)]
16. Shi, J.; Fu, Z.; Guo, W. Investigation of geometric effects on three-dimensional tunnel deformation mechanisms due to basement excavation. *Comput. Geotech.* **2019**, *106*, 108–116. [[CrossRef](#)]
17. Zhang, D.M.; Xie, X.C.; Li, Z.L.; Zhang, J. Simplified analysis method for predicting the influence of deep excavation on existing tunnels. *Comput. Geotech.* **2020**, *121*, 103477. [[CrossRef](#)]
18. Zucca, M.; Valente, M. On the limitations of decoupled approach for the seismic behaviour evaluation of shallow multi-propped underground structures embedded in granular soils. *Eng. Struct.* **2020**, *211*, 110497. [[CrossRef](#)]
19. Zhang, W.; Zhang, R.; Wang, W.; Zhang, F.; Goh, A.T. A multivariate adaptive regression splines model for determining horizontal wall deflection envelope for braced excavations in clays. *Tunn. Undergr. Space Technol.* **2019**, *84*, 461–471. [[CrossRef](#)]
20. Zhuang, Y.; Cui, X.; Hu, S. Numerical simulation and simplified analytical method to evaluate the displacement of adjacent tunnels caused by excavation. *Tunn. Undergr. Space Technol.* **2023**, *132*, 104879. [[CrossRef](#)]
21. Zheng, G.; Du, Y.; Cheng, X.; Diao, Y.; Deng, X.; Wang, F. Characteristics and prediction methods for tunnel deformations induced by excavations. *Geomech. Eng.* **2017**, *12*, 361–397. [[CrossRef](#)]
22. Liu, B.; Shao, C.; Wang, N.; Zhang, D. Influenced zone of deep excavation and a simplified prediction method for adjacent tunnel displacement in thick soft soil. *Appl. Sci.* **2023**, *13*, 4647. [[CrossRef](#)]
23. Wei, G.; Feng, F.; Hu, C.; Zhu, J.; Wang, X. Mechanical performances of shield tunnel segments under asymmetric unloading induced by pit excavation. *J. Rock. Mech. Geotech.* **2023**, *15*, 1547–1564. [[CrossRef](#)]
24. Zhou, N.; Vermeer, P.A.; Lou, R.; Tang, Y.; Jiang, S. Numerical simulation of deep foundation pit dewatering and optimization of controlling land subsidence. *Eng. Geol.* **2010**, *114*, 251–260. [[CrossRef](#)]
25. Li, M.G.; Xiao, X.; Wang, J.H.; Chen, J.J. Numerical study on responses of an existing metro line to staged deep excavations. *Tunn. Undergr. Space Technol.* **2019**, *85*, 268–281. [[CrossRef](#)]
26. Shi, J.; Zhang, X.; Chen, Y.; Chen, L. Numerical parametric study of countermeasures to alleviate basement excavation effects on an existing tunnel. *Tunn. Undergr. Space Technol.* **2018**, *72*, 145–153. [[CrossRef](#)]
27. Zheng, G.; Pan, J.; Li, Y.; Cheng, X.; Tan, F.; Du, Y.; Li, X. Deformation and protection of existing tunnels at an oblique intersection angle to an excavation. *Int. J. Geomech.* **2020**, *20*, 05020004. [[CrossRef](#)]
28. Yang, T.; Tong, L.; Pan, H.; Wang, Z.; Chen, X.; Li, H. Effect of excavation sequence on uplift deformation of underlying existing metro tunnel. *J. Perform. Constr. Facil.* **2021**, *35*, 04021003. [[CrossRef](#)]
29. Tanoli, A.Y.; Yan, B.; Xiong, Y.L.; Ye, G.L.; Khalid, U.; Xu, Z.H. Numerical analysis on zone-divided deep excavation in soft clays using a new small strain elasto–plastic constitutive model. *Undergr. Space* **2022**, *7*, 19–36. [[CrossRef](#)]
30. Guo, P.; Gong, X.; Wang, Y.; Lin, H.; Zhao, Y. Analysis of observed performance of a deep excavation straddled by shallowly buried pressurized pipelines and underneath traversed by planned tunnels. *Tunn. Undergr. Space Technol.* **2023**, *132*, 104946. [[CrossRef](#)]
31. Chen, Z.; Shi, Q.; Ji, D.; Luo, H.; Lin, J. Review of Research and Application of BIM-GIS Integration in the Civil Engineering Industry. In Proceedings of the International Conference on Construction and Real Estate Management 2023, Xi’an, China, 23–24 September 2023; Volume 2023, pp. 658–669.
32. Chen, D.W.; Zhou, J.L.; Duan, P.S.; Zhang, J.Q. Integrating knowledge management and BIM for safety risk identification of deep foundation pit construction. *Eng. Constr. Arch. Manag.* **2023**, *30*, 3242–3258. [[CrossRef](#)]
33. Zhang, Y.; Zhang, J.; Wang, C.; Ren, X. An integrated framework for improving the efficiency and safety of hydraulic tunnel construction. *Tunn. Undergr. Space Technol.* **2023**, *131*, 104836. [[CrossRef](#)]
34. Ursini, A.; Grazzini, A.; Matrone, F.; Zerbinatti, M. From scan-to-BIM to a structural finite elements model of built heritage for dynamic simulation. *Autom. Constr.* **2022**, *142*, 104518. [[CrossRef](#)]
35. Lai, H.; Deng, X. Interoperability analysis of IFC-based data exchange between heterogeneous BIM software. *J. Civ. Eng. Manag.* **2018**, *24*, 537–555. [[CrossRef](#)]

36. Cursi, S.; Martinelli, L.; Paraciani, N.; Calcerano, F.; Gigliarelli, E. Linking external knowledge to heritage BIM. *Autom. Constr.* **2022**, *141*, 104444. [[CrossRef](#)]
37. Tang, F.L.; Ma, T.; Guan, Y.S.; Zhang, Z.X. Parametric modeling and structure verification of asphalt pavement based on BIM-ABAQUS. *Autom. Constr.* **2020**, *111*, 103066. [[CrossRef](#)]
38. Fabozzi, S.; Biancardo, S.A.; Veropalumbo, R.; Bilotta, E. I-BIM based approach for geotechnical and numerical modelling of a conventional tunnel excavation. *Tunn. Undergr. Space Technol.* **2021**, *108*, 103723. [[CrossRef](#)]
39. Lin, C.J.; Wang, K.J.; Dagne, T.B.; Woldegiorgis, B.H. Balancing thermal comfort and energy conservation—A multi-objective optimization model for controlling aircondition and mechanical ventilation systems. *Build. Environ.* **2022**, *219*, 109237. [[CrossRef](#)]
40. Xie, P.; Zhang, R.J.; Zheng, J.J.; Li, Z.Q. Automatic safety evaluation and visualization of subway station excavation based on BIM-FEM/FDM integrated technology. *J. Civ. Eng. Manag.* **2022**, *28*, 320–336. [[CrossRef](#)]
41. Huang, H.; Ruan, B.; Wu, X.G.; Qin, Y.W. Parameterized modeling and safety simulation of shield tunnel based on BIM-FEM automation framework. *Autom. Constr.* **2024**, *162*, 105362. [[CrossRef](#)]

Disclaimer/Publisher’s Note: The statements, opinions and data contained in all publications are solely those of the individual author(s) and contributor(s) and not of MDPI and/or the editor(s). MDPI and/or the editor(s) disclaim responsibility for any injury to people or property resulting from any ideas, methods, instructions or products referred to in the content.